JOURNAL OF MATERIALS SCIENCE 19 (1984) 2203–2210

Tensile behaviour of two DO_3-ordered alloys: Fe_3Si and Fe–20 at% Al–5 at% Si

S. K. EHLERS, M. G. MENDIRATTA
Systems Research Laboratories, Inc., 2800 Indian Ripple Road, Dayton, Ohio 45440-3696, USA

The tensile behaviour, including fracture modes and deformation substructures, of two powder-produced DO_3-ordered alloys having compositions Fe–25 at% Si (Fe_3Si) and Fe–20 at% Al–5 at% Si, has been investigated from room temperature to 800° C. The brittle-to-ductile transition temperature for the Fe_3Si alloy occurred at a temperature between 500 and 550° C, while that of the Fe–20 at% Al–5 at% Si alloy was approximately room temperature. In both alloys fracture occurred by transgranular cleavage at room temperature, with the occurrence of an increasing proportion of intergranular cavitation with increasing temperature. At low strains plastic deformation occurred chiefly by movement of perfect superlattice dislocations which, with increasing strain, dissociated to produce next-nearest-neighbour antiphase boundary trails.

1. Introduction

The compound Fe_3Si possesses an ordered DO_3 crystal structure up to its melting temperature of 1250° C. It is known [1] that aluminium can substitute for silicon in Fe_3Si and still maintain the DO_3 order; however, increasing additions of aluminium for silicon result in a decrease in the temperature to which the DO_3 phase is stable. With increasing temperature a given DO_3 $Fe_3(Si, Al)$ compound transforms to another ordered phase having the B2 structure and, finally, disorders to the α-phase, providing a transformation sequence of $DO_3 \rightleftharpoons B2 \rightleftharpoons \alpha$.

Little is known regarding the mechanical properties of Fe_3Si, especially the high-temperature tensile behaviour. The compressive deformation behaviour of single-crystal and polycrystalline Fe_3Si has been studied [2, 3] up to 400° C; however, no work has been done to characterize the tensile deformation behaviour. Also, very little is known about the tensile deformation and fracture behaviour of $Fe_3(Si, Al)$ compounds.

A number of DO_3-ordered alloys having the chemical formula $Fe_3(Si, Al)$ are currently being studied to characterize the effect of varying silicon to aluminium proportions on the $DO_3 \rightleftharpoons B2$ phase transition temperature and on the tensile behaviour. This paper presents the results of an investigation on two of these alloys: Fe_3Si and Fe–20 at% Al–5 at% Si. Since Fe_3Si is an end member of these compounds, it is important to establish the baseline data for this alloy, especially the high-temperature behaviour. Presented for both alloys are the tensile behaviour as a function of temperature (room temperature to 800° C), the resulting fracture modes, and the deformation substructures.

2. Experimental procedure

The Fe_3Si and Fe–20 at% Al–5 at% Si alloys studied were fabricated using argon-atomized pre-alloyed powders (~ 80 mesh) having the compositions Fe–25 at% Al and Fe–25 at% Si; impurity content for these starting powders as obtained by wet chemical analysis is shown in Table I. The required amounts of powder for the Fe–20 at% Al–5 at% Si alloy were first mechanically blended in a steel V-mixer for 24 h. The powders were then canned in stainless/mild-steel extrusion cans and extruded at 1000° C at a ratio of 16:1. Details of the extrusion procedures and tensile-specimen design and machining are given elsewhere [4].

Prior to tensile testing, specimens were subjected to a homogenization anneal of 1000° C for 24 h

0022–2461/84 $03.00 + .12

TABLE I Impurity content of starting powders (wt %)

Element	Fe–25 at % Al	Fe–25 at % Si
C	0.01	0.01
N	0.004	0.004
O	0.032	0.012
Ni	0.5	0.05
Al	–	0.2
Si	0.003	–
Cr	0.1	0.005
Cu	0.05	0.04
W	0.05	0.1
Mo	0.01	0.015
Mn	0.005	0.004
Sn	0.01	0.001
Zn	–	0.05
Co	0.01	0.001

in vacuum, followed by ordering heat treatments of 850° C for 16 h for Fe_3Si and 700° C for 24 h for Fe–20 at % Al–5 at % Si in order to produce a high degree of DO_3 order. The $DO_3 \rightleftharpoons B2$ phase transition temperature (T_c) for the Fe–20 at % Al–5 at % Si alloy had been found to lie between 725 and 750° C; details of the T_c determination study are given elsewhere [5]. The microstructures of the annealed alloys were examined by metallography for grain size and structure and by transmission electron microscopy for the presence of dislocations and to confirm the presence of DO_3 order.

Tensile testing of the heat-treated specimens was performed in air using an Instron testing machine at a crosshead speed of 0.25 mm min^{-1}. For the Fe_3Si alloy, tests were run at temperatures ranging from room temperature to 800° C; specimens of Fe–20 at % Al–5 at % Si were tested from room temperature to 750° C. During testing, elongation was measured by a linear variable differential transformer (LVDT) mounted on the flanges of the test specimen. Engineering stress–strain curves were then generated from the load–elongation data recorded during testing.

The fracture surfaces of the test specimens were observed using an AMR-1000 scanning electron microscope in order to determine the fracture modes. Thin foils for transmission electron microscopy were prepared using the double-jet electropolishing technique with an electrolyte of one part nitric acid to two parts ethanol at a temperature of −40° C and current of ~ 20 mA. Thin foils prepared from slices cut parallel to and near the fracture surface were examined using a Philips EM300 TEM for dislocation structure and types of antiphase boundaries resulting from dislocation motion.

3. Results and discussion

3.1. Initial microstructure

Metallographic observation of longitudinal and transverse sections of the annealed Fe_3Si and Fe–20 at % Al–5 at % Si alloys indicated that the extrusion process and heat treatments previously described had produced an equiaxed grain structure in both cases. The resulting grain size in the Fe_3Si alloy was found to be ~ 18 μm and that of the Fe–20 at % Al–5 at % Si alloy to be ~ 25 μm. Electron-microprobe and chemical analyses of the extruded and heat-treated Fe–20 at % Al–5 at % Si alloy confirmed the aluminium content to be ~ 21 at % and the silicon content to be ~ 5 at %; microprobe data also indicated that iron, aluminium and silicon were uniformly distributed. Chemical analysis of Fe_3Si confirmed the silicon content to be ~ 24 at %.

TEM examination of thin foils of the annealed alloys revealed relatively dislocation-free grains possessing a high degree of DO_3 order. Fig. 1a is an electron micrograph showing a typical grain in the annealed Fe–20 at % Al–5 at % Si alloy in which practically no dislocations were observed. The intensity and sharpness of the [1 1 1] superlattice diffraction reflection in the [1 $\bar{1}$ 0]-zone-axis diffraction pattern (Fig. 1b) indicate the high degree of DO_3 order which has been achieved in the alloy after heat treatment.

3.2. Tensile behaviour

3.2.1. Fe_3Si

The engineering stress–strain curves for each test temperature are shown in Fig. 2. Fe_3Si was totally brittle at room temperature and failed at a low stress of ~ 400 MPa (58 x 10^3 psi). At 500° C, the fracture strength increased significantly to ~ 690 MPa; however, no macroplasticity was observed. At 550° C a 1% strain to fracture was exhibited, with a yield strength of 965 MPa (140 x 10^3 psi). Above 550° C the strength dropped rapidly, and a significant increase in ductility was observed. Thus, the brittle-to-ductile (B/D) transition temperature for this alloy appears to lie between 500 and 550° C.

The low fracture strength at room temperature indicates that fracture occurred prematurely, probably initiating from "Griffith"-type flaws. However, at 500° C a small amount of microplasticity may have taken place, thereby blunting the inherent flaws and consequently increasing the fracture strength. In previous studies of the

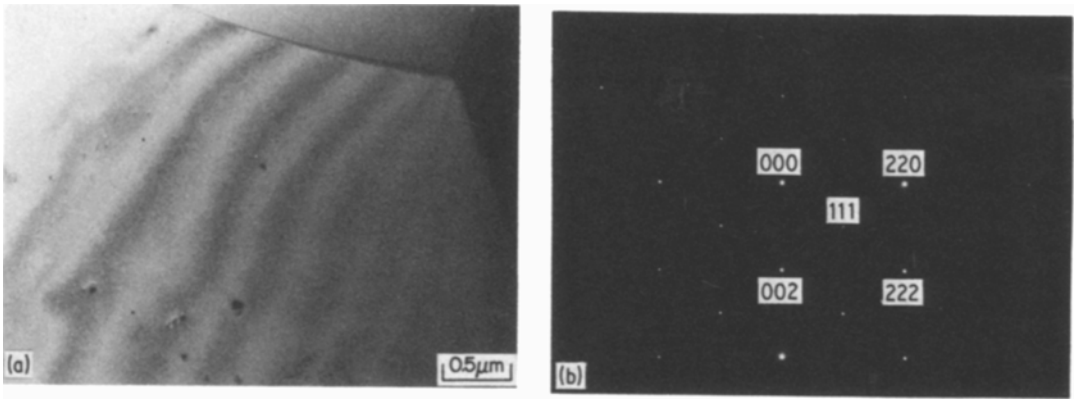

Figure 1 (a) Bright-field electron micrograph showing typical dislocation-free grain in the annealed Fe–20 at % Al–5 at % Si alloy (tilted to $g = [2\,2\,0]$ two-beam diffraction condition). (b) $[1\,\bar{1}\,0]$-zone-axis diffraction pattern.

compressive deformation behaviour [2, 3], the room-temperature yield strength of polycrystalline Fe_3Si having an average grain size of 500 μm was reported to be ~ 380 MPa (55×10^3 psi), with a small amount of plasticity occurring by nucleation and movement of superlattice dislocations. Based upon Hall–Petch-type grain-size dependence, the yield strength of the Fe_3Si in the present study having a grain size of ~ 18 μm should be approximately five times that of the coarser grain-size material (i.e. 5 x 380 MPa, or 1900 MPa). A yield strength of this magnitude would not likely be attained before initiation of fracture from the inherent flaws.

3.2.2. Fe–20 at % Al–5 at % Si

The engineering stress–strain curves for the Fe–20 at % Al–5 at % Si alloy tested from room temperature to 750° C are shown in Fig. 3. At room temperature, the alloy exhibited limited ductility (0.6% strain to fracture) and a yield strength of 800 MPa (116×10^3 psi). Fig. 4 shows the variation of 0.2% yield stress ($\sigma_{0.2}$), per cent elongation to fracture (ϵ_f), and per cent reduction

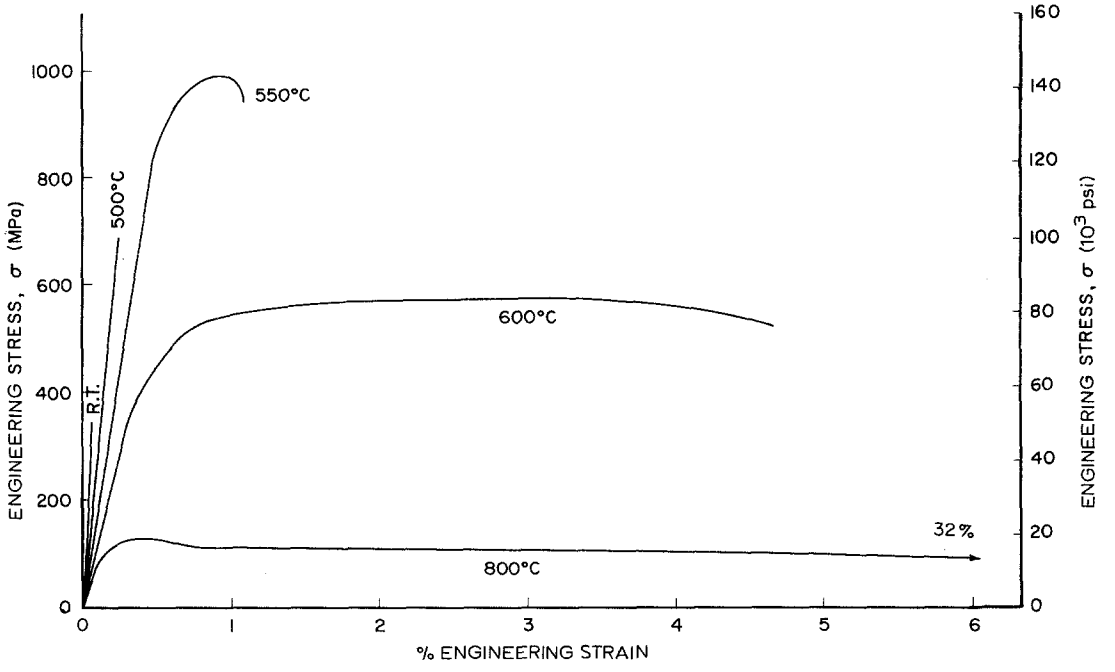

Figure 2 Engineering stress–strain curves for the Fe_3Si alloy at different test temperatures.

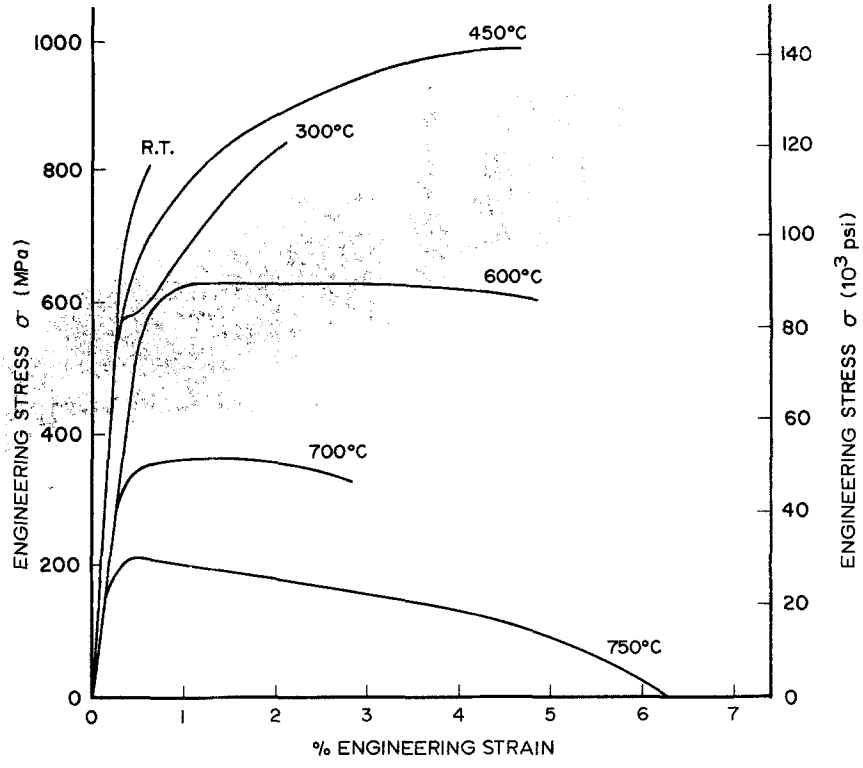

Figure 3 Engineering stress–strain curves for the Fe–20 at % Al–5 at % Si alloy at different test temperatures.

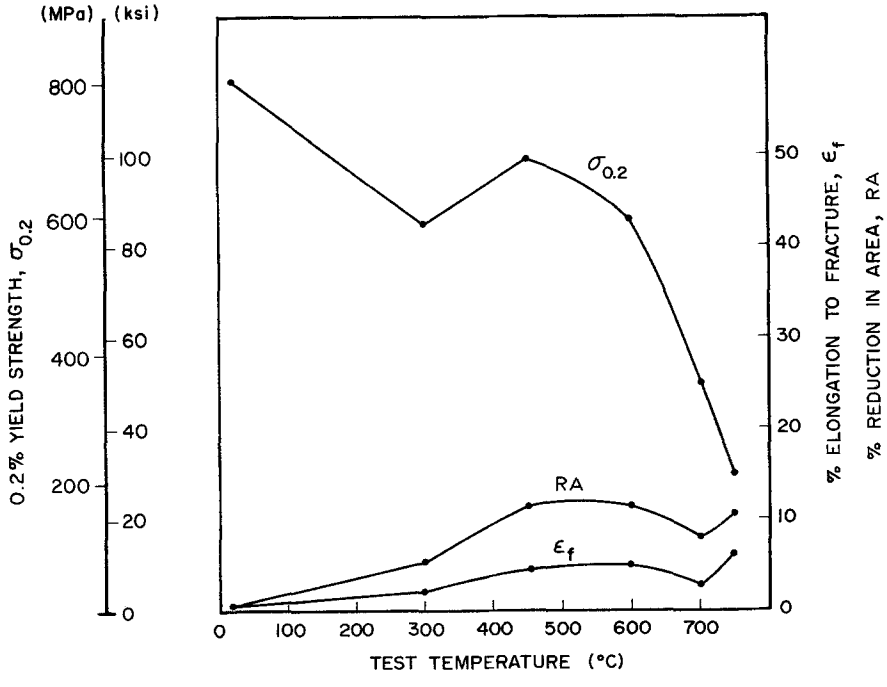

Figure 4 Variation of 0.2% yield stress ($\sigma_{0.2}$), per cent elongation to fracture (ϵ_f), and per cent reduction in area)RA) with test temperature for the Fe–20 at % Al–5 at % Si alloy.

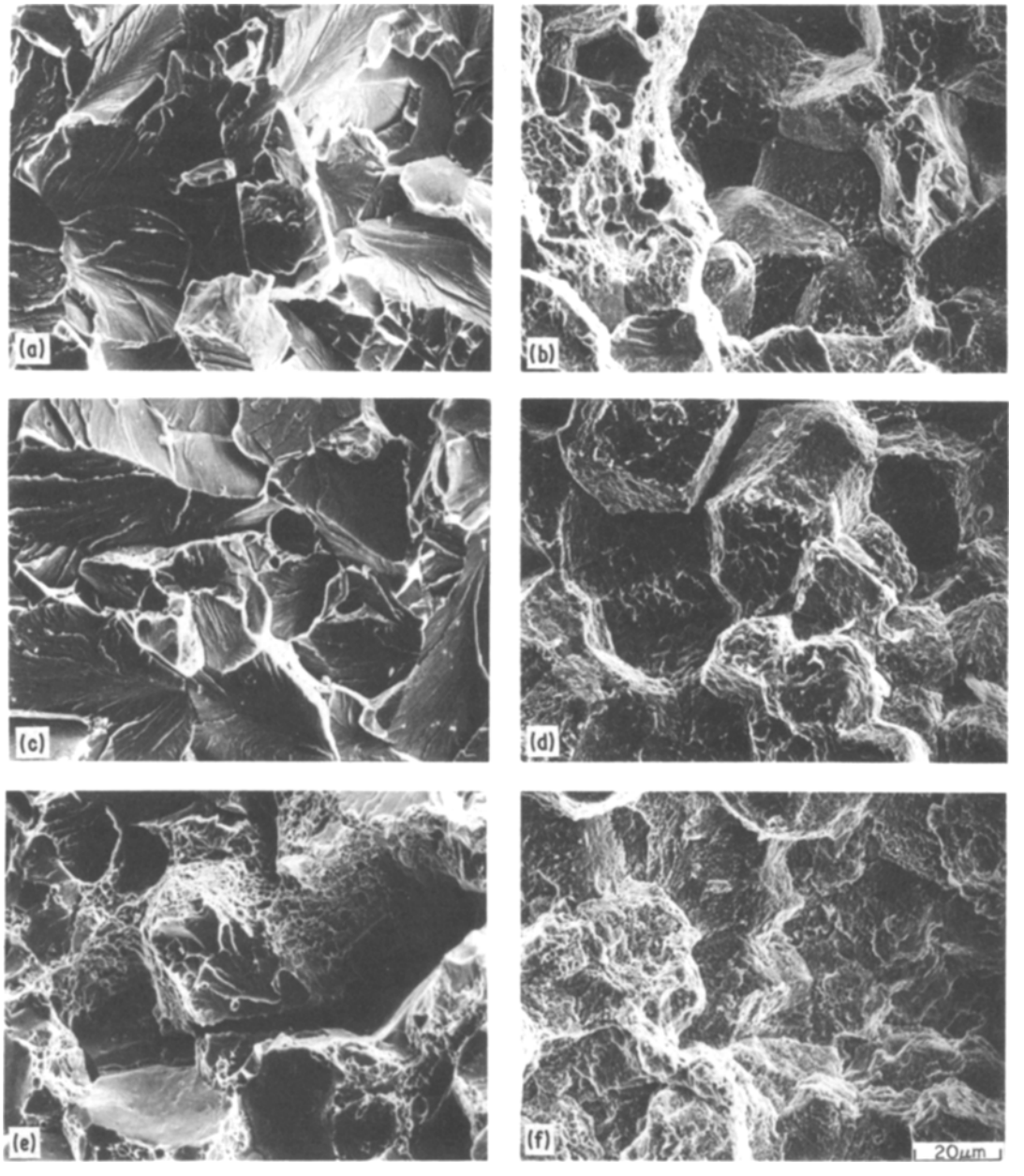

Figure 5 SEM fractographs for the alloy Fe–20 at % Al–5 at % Si illustrating fracture modes for each test temperature; (a) room temperature, (b) 600° C, (c) 300° C, (d) 700° C, (e) 450° C, and (f) 750° C.

in area (RA) with test temperature. A drop in yield strength occurs at a temperature of 300° C, but increases again at 450° C, followed by a continuous decrease to 750° C. The ductility of this alloy increases with temperature up to 600° C; at 700° C a drop in both the ϵ_f and the RA occurs, followed by an increase again at 750° C. In the Fe–20 at % Al–5 at % Si alloy, then, the B/D transition temperature appears to be approximately room temperature.

3.3. Fracture modes

Representative SEM fractographs of the Fe–20 at % Al–5 at % Si alloy for each test temperature are shown in Fig. 5. At room temperature and 300° C, the fracture mode was entirely transgranular cleavage, which is consistent with the fact that only a limited amount of ductility was observed at these temperatures for this alloy. With increasing test temperature, the fracture mode became mixed transgranular cleavage and inter-

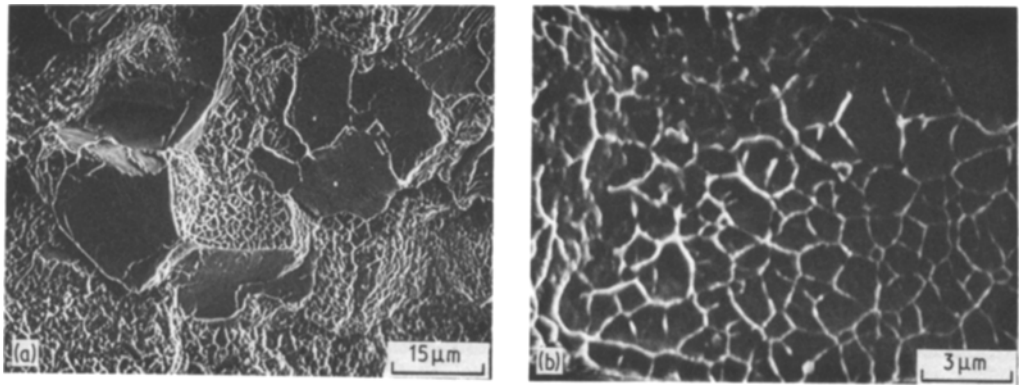

Figure 6 (a) SEM fractograph showing mixed-mode fracture in the Fe_3Si alloy at a test temperature of 600° C. (b) Higher magnification of same area as in (a) showing intergranular cavities in more detail.

granular fracture, accompanied by formation of cavities on the intergranular surfaces; the proportion of intergranular fracture and cavitation was observed to increase with increasing test temperature.

At 700° C, where a ductility loss was observed in this alloy, the fracture mode was entirely intergranular, with extremely small cavity-like features present on the intergranular facets. Generally, such a fracture mode is observed in alloys subjected to creep deformation, where it is believed that impurities segregate to the grain boundaries and aid in cavity nucleation. However, in this case, the strain rate was high, although the diffusion of some types of impurities may have been sufficiently rapid to play a role.

Fracture in Fe_3Si occurred in a similar manner as that in the Fe–20 at % Al–5 at % Si alloy. Below the B/D transition temperature (500 to 550° C), the fracture mode was entirely transgranular cleavage. With increasing temperature, the proportion of intergranular fracture and cavitation increased, as was observed in Fe–20 at % Al–5 at % Si. An example of this mixed-mode fracture in Fe_3Si is shown in Fig. 6, where the intergranular cavities are clearly seen at a test temperature of 600° C.

3.4. Deformation substructures

The possible superlattice-dislocation configurations in the DO_3 alloys and the two-beam TEM diffraction conditions needed to generate contrast from these configurations are given in a number of publications [2, 6]. A superlattice dislocation in a DO_3 alloy consists of four ordinary dislocations, each having a Burgers vector of $\frac{1}{4}a_0'\langle 1\,1\,1\rangle$ where a_0' is the lattice parameter of the superlattice and is double that of the corresponding disordered b c c lattice. The first (i.e. the leading) and second dislocations are separated by a nearest-neighbour antiphase boundary (NNAPB), the second and third by a next-nearest-neighbour antiphase boundary (NNNAPB), and the third and fourth again by a NNAPB. A small amount of ductility is possible if the superlattice dislocations can nucleate and move in the crystal (e.g. in Fe_3Si [2]); however, much more ductility can occur if the component dislocations can move freely and cross-slip because of the low APB energies and large separation distances (e.g. in Fe_3Al [6]).

In the present investigation, TEM examination of the deformed specimens of both alloys revealed that the onset of ductility occurred with the movement of superlattice dislocations having two-component dislocations of Burgers vectors $\frac{1}{2}a_0'\langle 1\,1\,1\rangle$ separated by NNNAPBs. Figs. 7a and b show the superlattice dislocations in Fe_3Si deformed at 550° C and in Fe–20 at % Al–5 at % Si deformed at room temperature, respectively. The observation of two-component superlattice dislocations in Fe_3Si is due to the very high NNAPB energy [2] such that separation between the first and second and between the third and fourth dislocations cannot be resolved. Although substitution of silicon with aluminium supposedly decreases the APB energies, the decrease in NNAPB energy is insufficient, even with 20 at % substitution; therefore, it was not possible to resolve a four-component superlattice dislocation in Fe–20 at % Al–5 at % Si.

It has been shown that in Fe_3Si deformed in compression, superlattice dislocations can nucleate

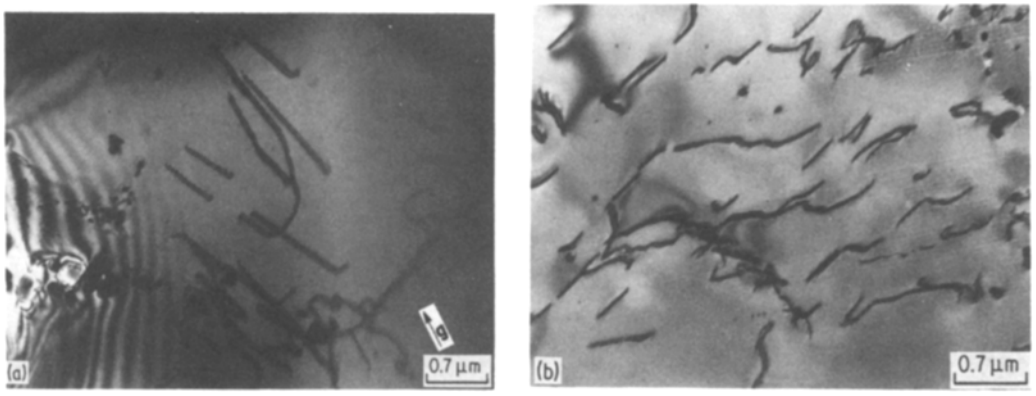

Figure 7 Electron micrographs showing superlattic dislocations of type $\frac{1}{2}a'_0\langle 1\,1\,1\rangle$ observed with $\mathbf{g} = [2\,2\,0]$. (a) Fe_3Si deformed at 550° C. (b) Fe–20 at % Al–5 at % Si deformed at room temperature.

and move, even at room temperature; however, these dislocations provide extremely high work-hardening due to Taylor-type locking [2], resulting in limited ductility. In the present study, the expected very high yield stress of the Fe_3Si due to small grain size and high work-hardening does not permit the occurrence of measurable tensile ductility at room temperature. Therefore, the mechanism of the B/D transition in Fe_3Si (at ~ 550° C) involves a sufficient decrease in the yield stress to permit blunting of inherent fracture-initiating flaws. In contrast, in the Fe–20 at % Al–5 at % Si alloy, the yield strength at room temperature is sufficiently low to provide some measure of ductility.

With increasing flow stress, the superlattice dislocations in both Fe_3Si and Fe–20 at % Al–5 at % Si dissociated to produce NNNAPB bands. These bands are shown in the dark-field TEM micrographs of Figs. 8a and b, respectively. It was observed that the dislocations cross-slipped extensively at 600° C for Fe_3Si and at 300° C for Fe–20 at % Al–5 at % Si. In the Fe–20 at % Al–5 at % Si alloy, no difference was observed in the character of dislocations for specimens deformed at 300 and 450° C; in both cases superlattice dislocations and NNNAPBs were observed. The increase in yield stress at 450° C over that for 300° C may be due to diffusion-assisted climb of leading dislocations of the superlattice dislocations out of their {1 1 0} slip planes and formation of APBs on {1 0 0}-type planes. Such a configuration occurs due to APB energy being lower on {1 0 0} planes than on {1 1 0} planes and has been proposed to explain an increase in yield strength with temperature in Fe_3Si [3] and Ni_3Al [7].

4. Conclusion

For the Fe_3Si alloy at room temperature, no ductility was observed and a low fracture strength

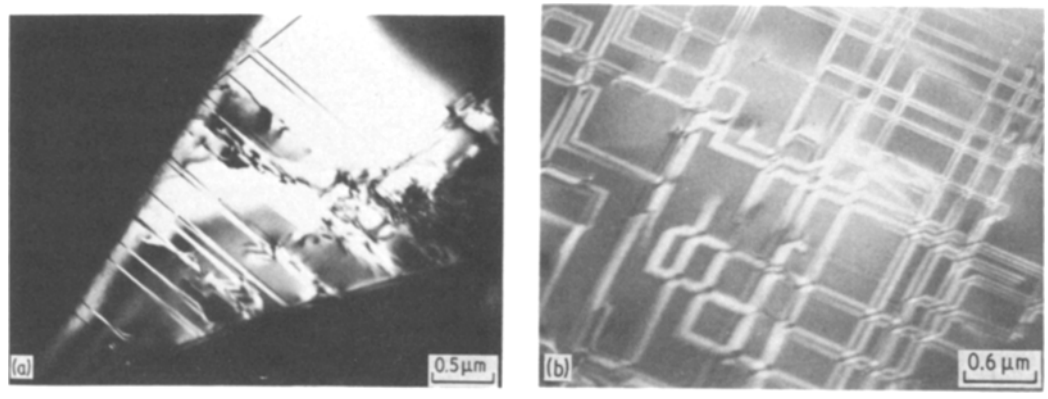

Figure 8 Dark-field electron micrographs ($\mathbf{g} = [1\,1\,1]$) showing NNNAPB bands formed by dissociation of superlattice dislocations. (a) Fe_3Si deformed at 550° C. (b) Fe–20 at % Al–5 at % Si deformed at room temperature.

of 400 MPa (58×10^3 psi) was exhibited. At 600° C, a good combination of strength (525 MPa) and ductility (4.5% strain to fracture) was observed. The B/D transition temperature was shown to lie between 500 and 550° C. Fracture in Fe_3Si occurred chiefly by transgranular cleavage up to the B/D transition temperature, with the occurrence of increasing proportions of intergranular cavitation with increasing test temperature. Deformation occurred chiefly by movement of perfect superlattice dislocations which then dissociated with increasing stress, leaving behind NNNAPB trails.

In the Fe–20 at % Al–5 at % Si alloy, limited ductility (0.6% strain to fracture) was exhibited at room temperature, with a yield strength of 800 MPa (116×10^3 psi). Therefore, the B/D transition temperature was approximately room temperature. Reasonable strengths were exhibited at higher temperatures, the yield strength being 593 MPa at 600° C and 345 MPa at 700° C. The fracture modes and deformation substructures in Fe–20 at % Al–5 at % Si were similar to those observed in Fe_3Si.

Acknowledgements

This research was supported in part by Air Force Contract F33615-81-C-5059. The authors wish to thank Dr Harry A. Lipsitt for helpful discussions of the manuscript and Mr Donald Adamson for technical assistance.

References

1. V. E. POLISHCHUK and Ya. P. SELISSKII, *Ukr. Fiz. Zh.* **14** (1969) 1722.
2. G. E. LAKSO and M. J. MARCINKOWSKI. *Trans. AIME* **245** (1969) 1111.
3. *Idem, Met. Trans.* **5A** (1974) 839.
4. H. A. LIPSITT, D. SHECHTMAN and R. E. SCHAFRIK, *ibid.* **6A** (1975) 1991.
5. M. G. MENDIRATTA and S. K. EHLERS, *ibid.* **14A** (1983) 2435.
6. M. J. MARCINKOWSKI and N. BROWN, *Acta Metall.* **9** (1961) 764.
7. P. A. FLINN, *Trans. Met. Soc. AIME* **218** (1960) 145.

Received 20 September
and accepted 29 September 1983